Assessment of CAPRI Predictions in Rounds 3–5 Shows Progress in Docking Procedures

Raúl Méndez,[1,2] Raphaël Leplae,[1] Marc F. Lensink,[1] and Shoshana J. Wodak[1,3]*

[1]*Service de Conformation de Macromolécules Biologiques et Bioinformatique, Centre de Biologie Structurale et Bioinformatique, Université Libre de Bruxelles, Bruxelles, Belgium*
[2]*Grup Biomatemàtic de Recerca, Institut de Neurociències, Unitat de Bioestadística, Facultat de Medicina, Universitat Autonòma de Barcelona, Bellaterra, Spain*
[3]*Structural Biology Program, Hospital for Sick Children, Toronto, Ontario, Canada*

ABSTRACT The current status of docking procedures for predicting protein–protein interactions starting from their three-dimensional (3D) structure is reassessed by evaluating blind predictions, performed during 2003–2004 as part of Rounds 3–5 of the community-wide experiment on Critical Assessment of PRedicted Interactions (CAPRI). Ten newly determined structures of protein–protein complexes were used as targets for these rounds. They comprised 2 enzyme–inhibitor complexes, 2 antigen–antibody complexes, 2 complexes involved in cellular signaling, 2 homo-oligomers, and a complex between 2 components of the bacterial cellulosome. For most targets, the predictors were given the experimental structures of 1 unbound and 1 bound component, with the latter in a random orientation. For some, the structure of the free component was derived from that of a related protein, requiring the use of homology modeling. In some of the targets, significant differences in conformation were displayed between the bound and unbound components, representing a major challenge for the docking procedures. For 1 target, predictions could not go to completion. In total, 1866 predictions submitted by 30 groups were evaluated. Over one-third of these groups applied completely novel docking algorithms and scoring functions, with several of them specifically addressing the challenge of dealing with side-chain and backbone flexibility. The quality of the predicted interactions was evaluated by comparison to the experimental structures of the targets, made available for the evaluation, using the well-agreed-upon criteria used previously. Twenty-four groups, which for the first time included an automatic Web server, produced predictions ranking from acceptable to highly accurate for all targets, including those where the structures of the bound and unbound forms differed substantially. These results and a brief survey of the methods used by participants of CAPRI Rounds 3–5 suggest that genuine progress in the performance of docking methods is being achieved, with CAPRI acting as the catalyst. Proteins 2005;60:150–169.
© 2005 Wiley-Liss, Inc.

INTRODUCTION

The biological function of gene products such as proteins and RNA is mediated through the interactions that they make with one another and with DNA. Characterizing these interactions in cellular systems and gaining understanding of their mechanism has therefore become a central theme in biology.[1,2] Recent genome-scale analyses indicate that in model organisms such as bacteria and yeast, the full set of interacting protein pairs—the interactome—may be several orders of magnitude larger than the set of protein-coding genes.[3–5] In humans, the larger number of proteins is expected to engage in hundreds of thousands of interactions, many of which involve large assemblies and play key roles in cellular function and disease.

Such assemblies are, however, still rather poorly represented in the Protein Data Bank (PDB). Structural genomics programs have so far focused on large-scale structure determination of individual gene products, but not on larger assemblies.[6,7] Although this is already changing, with new efforts combining crystallography, NMR, and cryoelectron microscopy being set up for analyzing multicomponent complexes, sampling of the interactome is likely to remain sparse for the near future, whereas the repertoire of individual protein structures will be increasingly well sampled.

Computational procedures capable of reliably generating structural models of multiprotein assemblies starting from the atomic coordinates of the individual components,

the so-called "docking" methods, should therefore play an important role in helping bridge the gap. But, as with other predictive approaches, objective tests are needed to monitor their performance. CAPRI, a community-wide experiment analogous to CASP,[8] was set up in 2001, with exactly this goal. In CAPRI, individual groups that develop docking procedures, predict the 3-dimensional (3D) structure of a protein complex from the known structures of the components. The predicted structure is subsequently assessed by comparing it to the experimental structure—the target—determined most commonly by X-ray diffraction, which is deposited with CAPRI prior to publication. The predictions are thus made blindly—without prior knowledge of the correct answer, and the evaluation is carried out by an independent team that has no knowledge of the identity of the predictors.

In the 4 years of CAPRI's existence, 5 prediction rounds have been performed on a total of 17 targets representing a spectrum of complexes. Rounds 1 and 2, which were completed in 2001–2002, had their results described previously.[9–11] Here we present those for Rounds 3–5, which were completed in 2003–2004. These latter 3 rounds initially included 12 targets, but 2 had to be cancelled, and predictions of another were interrupted prematurely, as the corresponding experimental structure was published by the authors before the deadline for submitting the predictions. The results presented here are for the remaining 9 targets. Those comprised an enzyme–inhibitor complex, 2 antigen–antibody complexes, 2 complexes involved in signal transduction pathways, 2 homo-oligomers, and a complex between 2 components of the cellulosome in bacteria.

For these targets, a total of 1866 models were evaluated, submitted by 30 groups, with each group providing at most 10 models per target. In comparison, a total of 465 predictions, submitted by 19 groups, were evaluated in the first 2 rounds of CAPRI. As was done previously, no limits were set on the source or type of additional information (homologous proteins, biochemical data on interacting residues) that predictors could use to guide their docking calculations.

The described evaluation is based on a number of criteria (Figure 1), most of which were previously agreed upon by the CAPRI management team and reapproved by the predictor groups during the second CAPRI evaluation meeting held in Gaeta (Italy), on December 8–10, 2004 (http://capri.ebi.ac.uk/). We present the results obtained for individual targets, as well as across predictor groups and across targets. Furthermore, we provide an overview of recent progress in docking procedures used by CAPRI participants, with emphasis on recent improvements and novel approaches, and on their likely impact on performance.

THE TARGETS

Predictions were evaluated for a total of 9 targets in CAPRI Rounds 3–5. Three additional targets were made available to predictors during Round 5 but were cancelled before the closing date for submitting predictions, because information about their crystal structures became available prematurely. Detailed information about the 9 evaluated targets can be found in Ref 12. These targets are denoted as T08–T19, reflecting the sequence at which they were made available to the successive rounds of CAPRI.

Targets T08 and T14 of Rounds 3 and 5, respectively, were complexes involved in signal transduction processes. T08 was a complex between the G3 domain of nidogen and a fragment of laminin containing 3 Epidermal Growth Factors (EGF) modules[13] (PDB entry: 1NPE). T14 was a complex between the protein phosphatase-1δ (PP1δ) catalytic subunit and the myosin phosphatase targeting subunit MYPT1 (PDB entry: 1S70), a regulatory subunit which confers substrate specificity to myosin phosphatase.[14] Both targets were of the bound–unbound category (Table I in Ref. 12), meaning that for 1 of the components, the predictors were given atomic coordinates from an independent study of the free protein, whereas for the other, they were given the atomic coordinates taken from the complex and randomly oriented. In T14, the unbound structure was in fact that of a related protein (PDB entry: 1FJM), requiring the use of homology modeling, which represented a new and further challenge for the prediction calculations.

The majority of the targets of CAPRI Rounds 3–5 were of the bound–unbound category, highlighting the difficulty of obtaining targets for which unbound structures are available for both components.

As in previous rounds of CAPRI, the 9 targets evaluated here cover a good range of biological systems with typical characteristics of protein complexes. The interface areas of the complexes are in the range usually encountered in protein complexes,[10,15] as seen in Table I in Ref. 12. Larger interface areas are buried in the homodimer (T09) and homotrimer (T10), and in the phosphatase–MYPT1 complex (T14). In the latter complex, the larger interface area is due to extended chain fragments from both proteins reaching out to interact with the neighboring subunit. The types of residues involved in the different interfaces (charged, polar hydrophobic) are also quite typical. Interestingly, the interfaces of T08, T09, T11, T12, and T14 involved an important fraction of hydrophobic groups (40–48%), whereas in T13, T18, and T19, this fraction was significantly lower (27–37%).

The 9 targets represented different levels of difficulty for the prediction programs, as discussed in detail in Janin[12] and Vajda.[16] Several factors determine this difficulty level. Although progress is being made in handling conformational changes in docking procedures, the difficulty of a target still very much depends on the magnitude and type of such changes in the unbound versus bound components.

Figure 1 illustrates the differences in conformation between the bound and unbound components in targets where these changes were significant. The backbone root-mean-square deviation (RMSD) of the bound versus unbound moieties, which is a measure of the conformational change, was largest (in excess of 10 Å) for the oligomeric targets (T09, T10). It was also substantial (10 Å) for the antigen moiety in T13, representing mainly the movement
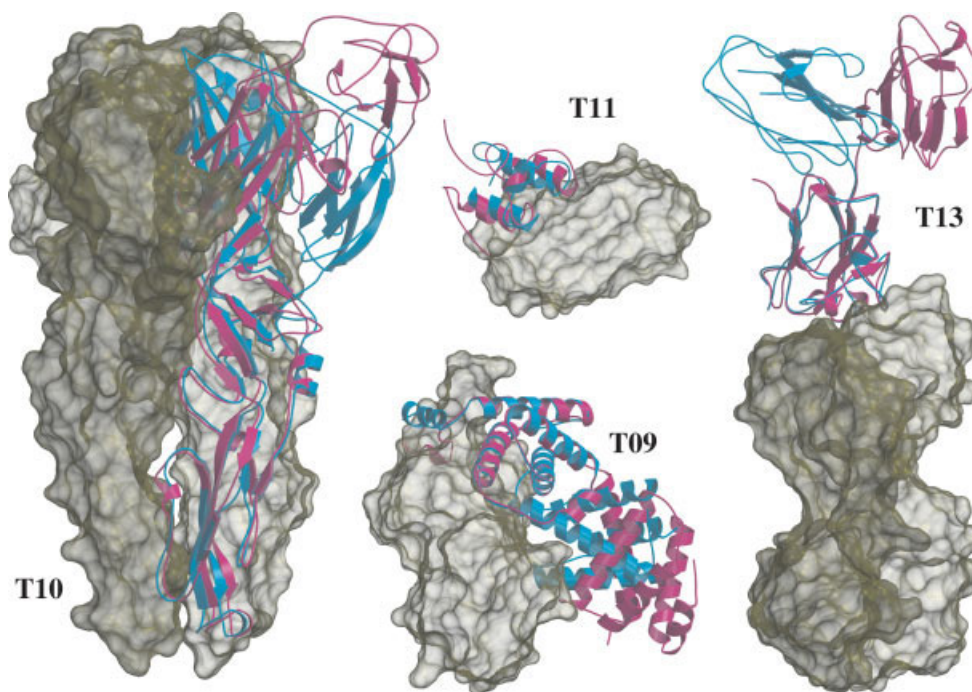
Fig. 1.   Conformation changes in targets of CAPRI Rounds 3–5. Bound chains are in cyan, and unbound chains in magenta, with the rest of the molecule drawn as a solid surface. Figure drawn with Molscript[17] and MSMS[18] rendered with Raster3D.[19] **T09:** LicT subunits in the wild-type (1TLV) and mutant (1H99) dimers. The RMSD of the backbone atoms is 12 Å after optimal superimposition. **T10:** subunit of the TBE virus protein E subunits in the low pH trimeric (1URZ) and dimeric form (1SVB). The RMSD of the backbone atoms is 11 Å after optimal superimposition. **T11:** dockerin in the bound (1OHZ) form is compared to the unbound NMR structure used as a template for homology modeling (1DAQ). The RMSD of the backbone atoms is 4.4 Å after optimal superimposition. **T13:** bound and uinbound (1KZQ) structures of SAG1. The RMSD of the backbone atoms is 10 Å after optimal superimposition.
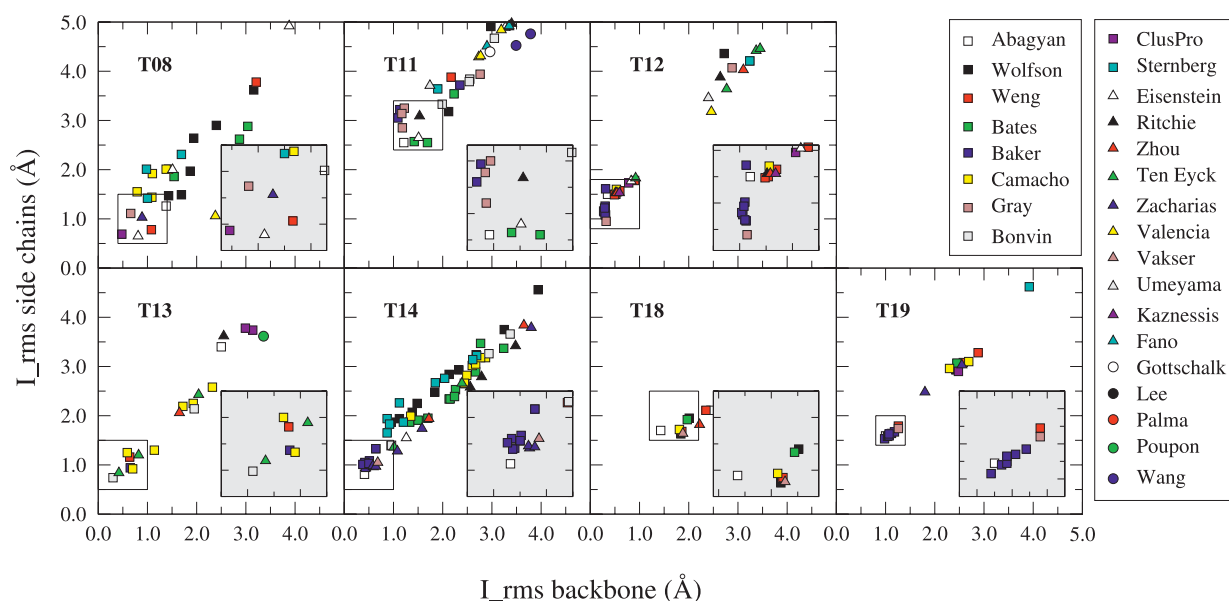
Fig. 3.   Interface side-chain and backbone prediction in CAPRI Rounds 3–5. The RMSD of interface side-chain in submitted models relative to the target structure atoms is plotted against the same quantity calculated for interface backbone. Incorrect models are omitted, and Target 10 is not shown due to the poor quality of the prediction. The inserts are zooms on the high-scoring regions of each graph. The best scores with a low I_rms for both the backbone and the side-chains, have been achieved by ClusPro (T08), Abagyan (T11, T14, T18), Gray (T12), Bonvin (T13), and Baker (T19). Legends are constructed following participant name's order in Table II, sorted by the number of predicted targets with at least 1 model acceptable or better.

Fig. 2. Schematic illustration of the quality measures used to evaluate the predicted models. For each target, we computed the number of residue–residue contacts between the receptor (R) and the ligand (L), and for each of the components, the number of interface residues. See text for the definition of the interface in each case. For each model, we computed the fractions f_{nat} of native and $f_{non-nat}$ of non-native contacts in the predicted interface. In addition we computed the RMSD of the backbone atoms of the ligand (L_rms), the misorientation angle θ_L and the residual displacement d_L of the ligand center of mass after the receptor in the model and experimental structures were optimally superimposed.[20] We also computed I_rms, the RMSD of the backbone atoms of the interface residues after they have been optimally superimposed.

of domain 2 (residues 133–253), and rather large (4.4 Å) for the dockerin moiety in T11. A related source of difficulty is when segments of the polypeptide chains, which are disordered in the unbound moiety (and hence have no atomic coordinates assigned to them), become ordered upon association. This sometimes requires modeling the structure of the missing segments, especially when the segments in question contribute to the interface. This was the case for residues 301–307 in the free phosphatase in T14.

In CAPRI Rounds 4 and 5, predictors faced a new and further challenge, that of applying homology modeling to derive the atomic coordinates of the unbound component

using as template a related 3D structure. This was the case for T11, T14, and T19, and the added difficulty arose from the deleterious effect that inaccurate atomic models might have on the docking results. Details on the sequence identity with the template structures and the sequence alignments that were given to predictors can be found on the CAPRI Web site (http://capri.ebi.ac.uk/). Another new challenge was presented by T09 and T10, where the unbound subunits had to be assembled into a homodimer and homotrimer, requiring the incorporation of symmetry constraints in the docking calculations.

For many targets, the difficulties described above were offset to some extent by information available from other sources on the protein regions that are likely to interact in the complex. As already emphasized in the first CAPRI evaluation report,[11] such information plays a very important role in guiding docking calculations, as well as filtering docking in solutions, and rare are the predictors that do not exploit it. For several of the targets analyzed here the available information pertained to data from biochemical and mutagenesis studies on active site residues, phosphorylation sites, or the binding region. For other targets, information on sequence conservation derived from multiple sequence alignments was also used with significant success, as will be illustrated below.

THE EVALUATION PROTOCOL

The parameters and criteria used to evaluate the quality of the predictions were exactly the same as in the evaluation of CAPRI Rounds 1–2. This reflects the wide consensus reached among predictors and the CAPRI management on the adequacy of the assessment protocol.

The various computed parameters and quality criteria are illustrated in Figure 2. In the following we present them briefly. Further details can be found in Méndez et al.[11]

Two quantities, f_{nat} and $f_{non-nat}$, were computed to quantify the quality of the predicted interactions at the interface. The former is defined as the number of native (correct) residue–residue contacts in the predicted complex divided by the number of contacts in the target complex. The latter is the fraction of non-native contacts, $f_{non-nat}$, defined as the number of non-native (incorrect) residue–residue contacts in the predicted complex divided by the total number of contacts in that complex. A pair of residues on different sides of the interface was considered to be in contact if any of their atoms were within 5 Å. A third quantity f_{IR}, defined as the fraction of native residues in the predicted interface of the receptor and ligand molecules, respectively, was computed to evaluate the extent to which a prediction correctly identified the interaction region, or "epitopes."

Several parameters were used to assess the global geometric fit between the 3D structures of the predicted and observed complexes. The L_rms, was computed as the RMSD of the ligand (the smaller of the 2 proteins) in the predicted versus target complexes after the receptors (the larger of the 2 proteins) were optimally superimposed.[20] Superimpositions were computed on backbone atoms (N, Cα, C, O). In addition we evaluated the residual rigid-body

rotation angle θ_L and the residual translation vector of the geometric center d_L required to superimpose the ligand molecules once the receptors have been superimposed.

To quantify the fit in the interface region, we computed the quantity I_rms, defined as the RMSD after optimal superimposition of the backbone atoms of interface residues only in the predicted versus target complexes. For this calculation, the interface residues in the target were redefined as those having at least 1 atom within 10 Å of an atom on the other molecule.

As previously described,[11] complexes exceeding the average number of atomic clashes by 2 standard deviations or more were not evaluated.

The quality of the predictions was assigned to 1 of 4 categories—high accuracy, medium accuracy, acceptable accuracy, and incorrect—according to the values of 3 parameters, f_{nat}, L_rms, and I_rms, as previously described.[11]

For targets where the unbound component had fragments with missing atomic coordinates, predictors had the choice between modeling them or ignoring them altogether. In the assessment, the backbone superimpositions always included the largest common chain fragment used by all participants. On the other hand, portions of the chains with the largest conformational changes were excluded from the superimposition calculations. However, in computing the residue contacts or interface residues, all the atomic coordinates of the submitted model were considered.

In assessing the predictions for the homotrimer (T10), 1 subunit was taken as the ligand, whereas the remaining 2 subunits were treated together as the receptor.

PREDICTION RESULTS AND DISCUSSION

This section describes the evaluation results obtained for the 9 targets presented in CAPRI Rounds 3–5, summarized in Table I. First we describe the prediction results for individual targets. This is followed by an overview of the results across predictor groups and targets. Values of all the quality measures computed on all the submitted predictions for each target can be found on the CAPRI website (http://capri.ebi.ac.uk/).

Prediction Results for Individual Targets
T08: nidogen-G3–laminin complex

The prediction results for this target are summarized in Table I(A). The top portion gives a general summary and the bottom portion lists the best of the acceptable or higher predictions obtained for this target by each group and their quality measures. Nineteen groups submitted a total of 179 predictions, of which 12 predicted models were not evaluated, as they had a larger than average number of clashes (see Table I footnote for details). Of the remaining 167 models, 2 were of high accuracy ($f_{nat} \geq 0.5$, L_rms ≤ 5 Å or I_rms ≤ 1 Å), 9 were of medium accuracy, and 16 were of acceptable accuracy ($f_{nat} < 0.3$). The 2 high-accuracy solutions, obtained respectively by the groups of Eisenstein and Gray, were of comparable quality, as seen from

TABLE I. CAPRI Prediction Results for Individual Targets

A. T08
Nidogen G3–Laminin complex

Predictor groups	19
Evaluated predictions	179
High accuracy(***)	2
Medium accuracy(**)	9
Acceptable(*)	16
Incorrect	140
Predictions with clashes	12
Average no. of clashes (SD)	30.69 (36.31)

Model no. (category)	Predictors	f_{nat}	$f_{non-nat}$	f_{IR-L}	$f_{IR\ R}$	N_{clash}	L_rms	I_rms	$\theta_L(°)$	$d_L(Å)$
1(***)	Eisenstein	0.7	0.3	0.8	1.0	19	6.4	0.8	23.0	5.8
2(***)	Gray	0.5	0.3	0.8	1.0	3	4.6	0.7	24.1	4.0
1(**)	Weng	0.5	0.7	0.7	0.8	5	10.4	1.1	44.1	9.3
3(**)	ClusPro	0.5	0.4	0.8	0.9	8	6.3	0.5	25.6	5.5
1(**)	Zacharias	0.4	0.6	0.7	0.8	19	7.0	0.9	28.6	5.3
10(**)	Camacho	0.4	0.7	0.8	0.9	10	13.2	1.4	47.1	11.0
1(**)	Abagyan	0.3	0.6	0.8	0.7	9	7.6	1.4	33.6	6.2
5(**)	Sternberg	0.3	0.6	0.4	0.6	24	8.7	1.7	37.4	7.2
6(**)	Wolfson	0.3	0.8	0.4	0.9	18	10.3	1.4	45.1	9.2
8(*)	Bates	0.2	0.7	0.3	0.6	17	11.3	1.5	49.6	8.3
2(*)	Valencia	0.1	0.8	0.5	0.7	33	10.0	2.4	42.0	8.7

B. T09
Wild-type LicT homodimer

Predictor groups	17
Evaluated predictions	164
High accuracy(***)	0
Medium accuracy(**)	0
Acceptable(*)	1
Incorrect	152
Predictions with clashes	11
Average no. of clashes (SD)	69.93 (91.31)

Model no. (category)	Predictors	f_{nat}	$f_{non-nat}$	f_{IR-L}	$f_{IR\ R}$	N_{clash}	L_rms	I_rms	$\theta_L(°)$	$d_L(Å)$
1(*)	Wolfson	0.2	0.9	0.7	0.7	16	9.4	10.7	31.2	8.0

C. T10
Trimeric form of the TBVE envelope protein

Predictor groups	20
Evaluated predictions	171
High accuracy(***)	0
Medium accuracy(**)	1
Acceptable(*)	3
Incorrect	158
Predictions with clashes	9
Average no. of clashes (SD)	119.16 (178.83)

Model no. (category)	Predictors	f_{nat}	$f_{non-nat}$	f_{IR-L}	$f_{IR\ R}$	N_{clash}	L_rms	I_rms	$\theta_L(°)$	$d_L(Å)$
10(**)	Bonvin	0.3	0.5	0.4	0.4	23	2.9	1.9	3.6	1.5
4(*)	Wolfson	0.2	0.8	0.5	0.5	232	9.3	5.5	15.6	5.6
2(*)	Abagyan	0.2	0.3	0.3	0.3	16	8.5	4.5	15.2	2.5
9(*)	Bates	0.1	0.6	0.4	0.4	80	9.6	6.5	13.9	5.0

TABLE I. (Continued)

D. T11
Cellulosome cohesin–dockerin complex.

Predictor groups	19
Evaluated predictions	190
High accuracy(***)	0
Medium accuracy(**)	11
Acceptable(*)	31
Incorrect	140
Predictions with clashes	8
Average no. of clashes (SD)	26.48 (37.47)

Model no. (category)	Predictors	f_{nat}	$f_{non-nat}$	f_{IR-L}	f_{IR_R}	N_{clash}	L_rms	I_rms	$\theta_L(°)$	$d_L(Å)$
9(**)	Baker	0.4	0.5	0.8	0.9	3	5.8	1.1	59.6	3.5
6(**)	Gray	0.4	0.5	0.8	0.8	4	6.1	1.2	61.4	3.8
10(**)	Bonvin	0.4	0.6	0.8	0.8	9	6.0	2.0	68.2	3.8
3(**)	Abagyan	0.3	0.5	0.7	0.8	5	6.0	1.2	56.8	3.8
7(**)	Umeyama	0.3	0.7	0.8	0.9	28	6.2	1.7	46.6	4.2
5(**)	Bates	0.3	0.6	0.7	0.6	10	7.5	1.7	65.8	5.0
8(**)	Ritchie	0.3	0.7	0.8	0.8	49	7.9	1.5	75.3	5.3
3(*)	Wolfson	0.3	0.7	0.8	0.7	28	12.3	3.0	62.0	9.9
4(*)	Weng	0.3	0.8	0.7	0.8	4	15.3	3.6	84.2	12.4
4(*)	Valencia	0.3	0.7	0.7	0.6	23	12.8	3.2	69.6	10.2
1(*)	Fano	0.3	0.8	0.6	0.8	49	14.5	3.3	91.5	11.5
6(*)	Sternberg	0.2	0.8	0.5	0.8	11	8.4	1.9	89.8	4.7
1(*)	Gottschalk	0.2	0.9	0.6	0.9	74	12.8	3.0	93.9	9.6
7(*)	Wang	0.2	0.8	0.7	0.6	11	15.5	3.5	72.2	12.5
9(*)	Eisenstein	0.1	0.9	0.6	0.7	21	12.4	1.5	155.7	7.8

E. T12
Cellulosome cohesin-dockerin complex.

Predictor groups	22
Evaluated predictions	214
High accuracy(***)	21
Medium accuracy(**)	0
Acceptable(*)	14
Incorrect	165
Predictions with clashes	14
Average no. of clashes (SD)	23.65 (32.83)

Model no. (category)	Predictors	f_{nat}	$f_{non-nat}$	f_{IR-L}	f_{IR_R}	N_{clash}	L_rms	I_rms	$\theta_L(°)$	$d_L(Å)$
9(***)	ClusPro	0.9	0.3	0.8	0.9	8	3.2	0.8	14.7	2.5
2(***)	Weng	0.9	0.2	0.9	0.9	3	2.7	0.6	10.5	2.3
3(***)	Zhou	0.9	0.1	0.8	0.9	22	1.1	0.5	7.5	0.4
7(***)	Kaznessis	0.9	0.2	0.9	0.9	2	1.7	0.6	8.8	1.1
8(***)	Baker	0.9	0.1	0.8	0.9	3	0.6	0.3	2.2	0.5
1(***)	Gray	0.9	0.1	0.8	0.9	3	1.0	0.3	2.9	0.9
8(***)	Camacho	0.9	0.2	0.9	0.9	2	1.4	0.5	6.9	1.0
1(***)	Abagyan	0.8	0.1	0.8	0.8	2	0.7	0.3	2.5	0.6
6(***)	Ritchie	0.8	0.1	0.7	0.9	9	1.9	0.5	8.5	1.5
5(***)	Ten Eyck	0.8	0.2	0.8	0.9	21	3.0	0.9	11.6	2.5
8(***)	Eisenstein	0.7	0.2	0.9	0.8	16	2.2	0.8	13.4	1.2
1(*)	Umeyama	0.5	0.7	0.8	0.9	43	7.3	2.4	42.1	4.3
5(*)	Valencia	0.2	0.2	0.5	0.4	10	6.2	2.5	23.6	5.3
7(*)	Wolfson	0.2	0.7	0.7	0.7	33	8.4	4.1	60.3	2.6
4(*)	Sternberg	0.2	0.8	0.6	0.9	12	6.4	3.2	42.7	3.1
8(*)	Bates	0.1	0.8	0.5	0.7	20	9.5	4.3	65.3	4.3

TABLE I. (Continued)

F. T13
SAG1–antibody complex

Predictor groups	21
Evaluated predictions	210
High accuracy(***)	6
Medium accuracy(**)	6
Acceptable(*)	7
Incorrect	178
Predictions with clashes	13
Average no. of clashes (SD)	29.73 (39.24)

Model no. (category)	Predictors	f_{nat}	$f_{non\text{-}nat}$	$f_{IR\text{-}L}$	$f_{IR\ R}$	N_{clash}	L_rms	I_rms	$\theta_L(°)$	$d_L(Å)$
1(***)	Weng	0.9	0.3	0.9	1.0	10	2.6	0.6	5.3	2.2
1(***)	Bonvin	0.8	0.1	0.9	1.0	5	3.8	0.3	7.8	3.2
5(***)	Ten Eyck	0.8	0.4	0.9	0.9	63	5.6	0.8	13.4	4.6
10(***)	Camacho	0.7	0.2	0.8	0.9	4	3.5	0.6	8.7	3.0
9(**)	Zhou	0.5	0.6	0.9	1.0	60	7.1	1.6	21.5	5.7
5(**)	Baker	0.5	0.3	0.9	0.9	1	2.4	0.7	8.4	1.2
7(*)	Poupon	0.3	0.6	0.7	0.8	9	16.1	3.4	42.1	11.3
6(*)	Abagyan	0.2	0.7	0.7	0.8	6	11.1	2.5	43.3	4.0
6(*)	Ritchie	0.1	0.7	0.6	0.7	12	14.4	2.5	52.3	7.4
2(*)	ClusPro	0.1	0.8	0.5	0.6	3	17.4	3.1	30.5	13.4

G. T14
Protein Serine/Threonine Phosphatase-1–Myosin Phosphatase targeting subunit 1 complex

Predictor groups	25
Evaluated predictions	250
High accuracy(***)	16
Medium accuracy(**)	20
Acceptable(*)	32
Incorrect	173
Predictions with clashes	9
Average no. of clashes (SD)	52.28 (66.45)

Model no. (category)	Predictors	f_{nat}	$f_{non\text{-}nat}$	$f_{IR\text{-}L}$	$f_{IR\ R}$	N_{clash}	L_rms	I_rms	$\theta_L(°)$	$d_L(Å)$
1(***)	Abagyan	0.6	0.1	0.6	0.8	32	0.6	0.4	0.7	0.5
1(***)	Baker	0.6	0.1	0.6	0.8	10	0.9	0.5	2.7	0.3
2(***)	Zacharias	0.6	0.2	0.6	0.8	11	1.2	0.6	2.1	0.9
1(***)	Bonvin	0.6	0.3	0.7	0.8	11	2.3	1.0	2.2	2.2
8(***)	Weng	0.5	0.2	0.6	0.8	12	3.8	0.9	6.2	2.9
4(**)	Vakser	0.5	0.2	0.5	0.8	37	3.1	0.7	4.5	2.5
3(**)	Bates	0.5	0.3	0.5	0.7	14	2.6	1.3	6.0	1.6
6(**)	Wolfson	0.5	0.3	0.5	0.7	67	3.9	1.1	7.5	2.7
9(**)	Sternberg	0.5	0.3	0.6	0.8	23	4.5	0.9	6.2	3.7
9(**)	Ten Eyck	0.5	0.3	0.5	0.7	60	4.4	1.0	6.5	3.8
3(**)	Camacho	0.4	0.3	0.4	0.7	8	5.8	1.4	9.3	4.2
6(*)	Ritchie	0.4	0.6	0.7	0.6	181	8.9	3.5	16.1	7.3
1(**)	Eisenstein	0.3	0.2	0.6	0.6	31	5.3	1.3	6.5	4.6
1(*)	Zhou	0.3	0.3	0.5	0.6	16	6.5	1.7	15.4	4.6

H. T18
TAXI–Niger xilanase complex

Predictor groups	26
Evaluated predictions	252
High accuracy(***)	0
Medium accuracy(**)	6
Acceptable(*)	4
Incorrect	232
Predictions with clashes	10
Average no. of clashes (SD)	41.79 (61.94)

TABLE I. (Continued)

Model no. (category)	Predictors	f_{nat}	$f_{non-nat}$	f_{IR-L}	$f_{IR\ R}$	N_{clash}	L_rms	I_rms	$\theta_L(°)$	$d_L(\text{Å})$
2(*)	Zhou	0.9	0.6	0.9	0.9	85	6.8	2.2	21.1	5.2
5(**)	Vakser	0.9	0.5	1.0	1.0	110	5.1	1.9	15.8	3.9
1(**)	Weng	0.9	0.5	1.0	1.0	10	5.5	1.9	16.1	4.4
8(**)	Camacho	0.9	0.6	1.0	1.0	18	5.0	1.8	13.6	4.1
10(**)	Bates	0.8	0.6	1.0	1.0	101	5.0	2.0	15.2	3.9
3(**)	Wolfson	0.8	0.5	0.9	0.9	90	5.4	1.8	17.9	3.8
9(**)	Abagyan	0.7	0.6	0.9	0.8	92	3.0	1.4	6.4	2.6

I. T19
Ovine Prion–Fab complex

Predictor groups	24
Evaluated predictions	236
High accuracy(***)	1
Medium accuracy(**)	10
Acceptable(*)	9
Incorrect	204
Predictions with clashes	12
Average no. of clashes (SD)	35.69 (45.69)

Model no. (category)	Predictors	f_{nat}	$f_{non-nat}$	f_{IR-L}	$f_{IR\ R}$	N_{clash}	L_rms	I_rms	$\theta_L(°)$	$d_L(\text{Å})$
4(**)	Abagyan	0.7	0.3	1.0	0.9	80	4.1	1.0	18.7	2.9
1(***)	Baker	0.7	0.1	0.9	0.8	10	2.5	1.0	7.3	1.9
2(**)	Gray	0.6	0.1	0.7	0.8	10	3.6	1.3	11.6	2.9
9(**)	Zacharias	0.6	0.1	0.7	0.6	6	5.3	1.8	18.2	4.1
8(**)	Weng	0.6	0.3	0.8	0.8	6	4.7	1.3	13.4	3.9
2(*)	Wolfson	0.5	0.6	0.8	0.9	76	5.3	2.4	28.9	2.0
8(*)	Bates	0.4	0.5	0.7	0.9	35	5.6	2.4	30.2	1.0
3(*)	Camacho	0.4	0.5	0.8	0.7	5	7.4	2.3	32.5	3.8
9(*)	Sternberg	0.3	0.7	0.8	0.7	17	15.2	3.9	59.2	10.6
2(*)	ClusPro	0.3	0.5	0.7	0.7	1	6.9	2.5	33.2	3.2

Sections (a)–(i) of this Table are devoted to the results for individual targets 08–19. Each section is divided into 2 parts. The top part provides a general summary of the predictions and the bottom part lists the key parameters of the best predictions ranked as acceptable or higher submitted by each group.

The submitted predictions were divided into 4 categories as detailed in the text. Predictions with a number of clashes exceeding a defined threshold were not evaluated. Clashes were defined as those between 2 non-hydrogen atoms on each side of the interface whose distance was less than 3Å. The threshold was taken as 2 standard deviations plus the average of the number of clashes in all the predictions submitted for a given target.

Detailed results for the best predictions for each participant, which were of acceptable quality or better (bottom), were ranked as indicated in Figure 2. Column 1 lists the model number (1–5) and the rank of the prediction, high accuracy (***), medium accuracy (**), and acceptable (*). Column 2 lists the participant groups in order of decreasing native contact fraction f_{nat} (Column 3). Column 3 lists the fraction of non-native contacts $f_{non-nat}$, defined as the number of non-native contacts over the total number of contacts in the predicted complex. $f_{IR\_L/R}$ is defined as the number of native residues in the predicted interface over the total number of interface residues in the target, computed for both the R (receptor) or L (ligand) molecules. Column 7 ($N_{clashes}$) lists the number of atomic clashes in the predicted complex. Columns 8 and 9 list the rms values. L_RMS is the backbone rms (Å) of the ligand molecules in the predicted versus the target complexes after the receptor moieties have been superimposed. The I_RMS is the interface rms (Å) computed by superimposing only the backbone of the interface residues from the target complex onto their counterparts in the predicted complex. The last 2 columns list the residual rigid-body rotation (θ_L) and translation (d_L) of the ligand in the predicted versus the target complexes after the corresponding receptor molecules have been superimposed. For further details on how the various parameters were computed, see the text.

the values of different quality measures in Table I(A). Both correctly predicted all the interface residues, but the model from the Gray group had a particularly low number of clashes. The medium-quality models display a somewhat wider range of values for the quality measures, often with a large fraction of non-native contacts ($f_{non-nat}$ = 0.7–0.8). Not surprisingly, $f_{non-nat}$ was generally high (0.8–0.9) and f_{nat} low (0.1) in the so-called acceptable predictions. Two other sets of values are listed in the leftmost columns of Table I: θ_L, the ligand misorientation and d_L, the displacement of the ligand in the predicted

versus experimental structures (see legend of Fig. 2). We see that in both the high- and medium-accuracy models the ligand is misoriented in the predicted models by about 20–47° and its center is displaced by about 4–9 Å. This highlights the fact that models with well-predicted interfaces can still deviate quite significantly in their global geometry from the correct solution.

Overall, at least 1 acceptable model (or better) was obtained by 11 out of the 19 groups that submitted predictions. This is a satisfactory result considering that the laminin fragment comprised 3 similar EGF modules,

but available biochemical information indicated that the middle EGF module was primarily involved in the interactions.

T09: wild-type LicT homodimer

T09 was one of the most difficult targets of Rounds 3–5. It involved the prediction of a homodimer using the structure of a subunit of a double mutant (H207D/H269D), which forms a different dimer, and furthermore differs substantially in conformation (backbone RMSD of 12 Å) from the bound form. It is therefore not too surprising that the prediction results for this target were very poor, with only 1 acceptable model obtained by the group of Wolfson out of a total of 164 models submitted by 17 groups [Table I(B)]. Although the computed model is far from accurate (f_{nat} = 0.2, $f_{non-nat}$ = 0.9, L_rms ≥ 9 Å, etc.) this is a quite remarkable result.

T10: trimeric form of the tick-borne encephalitis virus (TBEV) envelope protein

This target offered very similar challenges to T09. It also involved the prediction of a homotrimer starting from the structure of a subunit from a dimer crystallized at a different pH and adopting a substantially different conformation (backbone RMSD of 11 Å). To help the predictors, they were invited to ignore the C-terminal domain of the subunit (residues 291–401).

Of the total of 171 models submitted by 20 groups, 4 models submitted by 4 different groups were of acceptable quality or better [Table I(C)]. The only medium-accuracy model was obtained by the group of Bonvin. It correctly predicted more than 30% of the interface contacts with about 40% non-native contacts, a L_rms < 3 Å, and I_rms < 2 Å. The 3 acceptable models predicted less than 20% of the native contacts and had much larger RMSD values.

Interestingly, we see that these models have significantly lower values for the ligand misorientation angle θ_L(~4–16°) and ligand displacement distance d_L(1.5–6 Å) than the higher quality models obtained for T08, where values for θ_L range between 23° and 100° and those for d_L range between 4 Å and 16 Å.[†]

T11 and T12: cohesin–dockerin complex of the cellulosome

The prediction results obtained for these 2 targets are summarized in Table I(D and E), respectively. Not surprisingly, they are significantly better for the bound–unbound (T12) than the unbound version (T11) of the target. No high accuracy model was produced for T11, whereas a total of 21 models, representing about 10% of all the submitted models of T12, are of high accuracy. In contrast, 11 medium-accuracy and 31 acceptable predictions were obtained for the more difficult T11; T12 had no medium-accuracy and only 14 acceptable predictions. This suggests that in easier targets, in which the conformations of the

bound and unbound components are similar, docking methods tend to produce either high-accuracy solutions or completely unrelated, incorrect ones.

The 11 participants who produced high-accuracy models for T12 were the automatic server ClusPro and the groups of Weng, Zhou, Kaznessis, Baker, Gray, Camacho, Abagyan, Ritchie, Ten Eyck, and Eisenstein. These models had at least 70% of the native contacts in the predicted interface. They also had low L_rms and I_rms values, indicating that the overall position of the ligand and the positions of interface residues were very close to those found in the target.

The 7 best medium-accuracy models of T11 were those by the groups of Baker, Gray, Bonvin, Abagyan, Umeyama, Bates, and Ritchie. Thus, several of the groups that produced medium-accuracy predictions for the more difficult T11 also produced high-quality models for the easier T12. It is rather satisfying to see that, for both targets, the proportion of groups that produced acceptable models (or better) was quite high—15 out of 19 groups for the more difficult T11, and 16 out of 22 groups for T12.

T13: SAG1-FAB complex

This can be considered as a difficult target given the large difference in conformation (~10 Å RMSD) between the bound and unbound forms of the SAG1 antigen molecule. However, in this case, the conformational difference had only a marginal impact if any at all, on the docking calculations, because it represents mainly a rigid-body movement of the 2 loosely interacting SAG1 domains relative to one another. Moreover, the interaction with the antibody fragment is mediated entirely by one of the domains (D1) involving a region on the opposite side from the domain–domain interface. As for most antigen–antibody complexes, the majority of the predictors assumed that the antibody interacts via its complementarity determining regions (CDRs) and used this information to constrain their calculations.

Inspection of Table I(F) reveals that 10 out of the total of 21 groups that submitted predictions produced models of acceptable accuracy or better. Of those 4 groups (Weng, Bonvin, Ten Eyck, and Camacho) produced high-accuracy models, with between 70% and 90% of the native interactions correctly predicted, a reasonably low fraction of non-native contacts (11–40%) and I_rms values of ≤ 1 Å. The ligand RMSDs were computed considering domain 1 of the SAG1 molecule as the receptor molecule and the FAB fragment as the ligand.

Interestingly, for this target, the number of high-, medium-, and acceptable-accuracy models was about the same (6, 6, and 7, respectively).

T14: protein Ser/Thr phosphatase-1- MYPT1 complex

The difficulty for this target stemmed from the fact that the unbound structure of the phosphatase 1δ had to be modeled from the structure of the closely related phosphatase 1α isoform. The backbone of this related structure differed little (< 1Å RMSD) from that of the bound form, however, except that it was missing the coordinates for the

---

[†]Because of the size and shape of the ligand subunit.

C-terminal fragment (residues 301–307), which becomes structured in the complex by making extensive contacts with the MYPT1 moiety. Predictors were, on the other hand, exploiting information available from biochemical studies on regions of the phosphatase moiety (mainly on active site residues) and of the MYPT1 molecule that participates in the interaction.

Inspection of Table I(G) reveals that the prediction results for this target are among the best obtained for all 3 rounds evaluated here. Sixteen out of the 25 groups submitting predictions produced models that were acceptable, or better. Of those, 5 groups (Abagyan, Baker, Zacharias, Bonvin and Weng), produced at least 1, and often more than 1, high-accuracy models, and 7 groups collectively produced 20 medium-accuracy models. Interestingly, modeling the missing segment, as some groups did, was in general not helpful, since few if any groups were able to do it correctly, confirming that correct modeling of backbone conformation is still a major roadblock.

T18: xylanase–TAXI 1 complex

This target was a typical enzyme–inhibitor complex for which predictors had to perform bound–unbound docking, with the unbound xylanase structure displaying small differences (backbone RMSD < 1 Å), with that of its bound counterpart.

The results listed in Table I(H) show, however, that only a small fraction of the predictor groups—7 out of a total of 26—produced acceptable (or better) predictions. Six of those (Abagyan, Bates, Camacho, Vakser, Wolfson, and Weng) submitted at least 1 medium-accuracy solution. Several of the models had most of the native contacts identified (70–90%) in the predicted interface, but this interface also contained a large fraction of false positives ($f_{non-nat} > 50\%$), and in all cases the I_rms values were < 1 Å.

Of the 252 models submitted for this target, none was of high accuracy, 6 were of medium accuracy, and only 4 were acceptable.

This is on the whole a disappointing result for what seemed to be an easy target. It suggests that the docking procedures were not efficient enough in sampling contacts with the TAXI inhibitor, an inactive homolog of aspartate proteases, which is a rather large molecule (300 residues).

T19: ovine prion–FAB complex

This was the second antigen–antibody target for which predictions were evaluated here. The structure of the unbound prion ovine antigen had to be derived by homology modeling from the NMR structure of the globular domain of its human counterpart. The backbone structure of the latter differed relatively little, however, from that of the bound ovine protein (1.6 Å RMSD).

Inspection of Table I(I), reveals that 10 of the 24 groups that submitted predictions for this target produced models that were of acceptable quality or better. Of those, only 2 groups Baker and Abagyan, submitted 1 model each that was, respectively, of high- and near-high accuracy.

Of the 3 targets for which homology modeling was performed on the unbound component, this was the one with the lowest success rate.

Prediction Results Across Predictor Groups and Targets

Table II summarizes the prediction results for all 9 targets in CAPRI Rounds 3–5 obtained by all groups that submitted at least 1 prediction ranking as acceptable or better. The listed results represent only the best prediction obtained by each group for each target. Thus, if a group submitted 2 acceptable predictions and 1 high-accuracy prediction for a given target, only the high-accuracy result is listed. For a full account of the results obtained by each group the reader is referred to the CAPRI website (http://capri.ebi.ac.uk/).

In total, 30 groups submitted predictions for at least 1 target in Rounds 3–5. Of those, 24 have an entry in Table II, which upon inspection reveals that all targets were predicted by at least 1 group. This clearly represents progress in comparison with the results reported previously for CAPRI Rounds 1–2,[11] where 2 out of a total of 7 targets had no correct prediction submitted by any group. One should note, however, that the failure to predict these targets was primarily due to inappropriate use of prior knowledge in biasing the docking calculations.

We see, moreover, that even very difficult targets, such as T09 and T10, where the components undergo substantial conformational changes and prediction methods faced new challenges such as docking subunits into a symmetrical assembly, acceptable predictions, or better, were obtained. For T09, one acceptable model was obtained by the group of Wolfson, whereas for T10, 3 acceptable and 1 medium-accuracy prediction were obtained by 4 independent groups. For other targets, which presented varying degrees of difficulty, several correct predictions, ranging in accuracy from acceptable to high, were obtained by several groups. A record number of groups submitted correct predictions (a total of 16, of which 11 submitted high-accuracy models) for T12, the unbound–bound version of the cohesin–dockerin complex. Interestingly, for T11, the unbound–unbound version of the cohesin–dockerin complex, where homology modeling had to be performed on the dockerin moiety, 15 groups submitted correct predictions, nearly the same number as for T12, but those included only 7 medium-accuracy models, reflecting the problem of dealing with medium-range conformational changes (4.4 Å RMSD).

Four of the remaining 5 targets had between 10 and 14 groups submitting correct predictions, which most often included a few (1–4) high-accuracy models. The scores for T18 were somewhat lower, with only 7 groups providing correct predictions, but the majority of these models (6) were of medium accuracy.

Table II also allows us to assess the success rate of individual groups, although this is a difficult and possibly controversial undertaking, because the number of evaluated targets remains much too small for drawing conclusions on a statistically significant basis.

TABLE II. Summary of Docking Predictions

Predictor group	T08	T09	T10	T11	T12	T13	T14	T18	T19	Predictor summary
Abagyan	**	0	*	**	***	*	***	**	**	8/4**/2***
Wolfson	**	*	*	*	*	0	**	**	*	8/3**
Weng	**	0	0	*	***	***	***	**	**	7/3**/3***
Bates	*	0	*	**	*	0	**	**	*	7/3**
Baker	—	0	0	**	***	**	***	0	***	6/2**/4***
Camacho	**	0	0	0	***	***	**	**	*	6/3**/2***
Gray	***	—	—	**	***	0	0	0	**	5/2**/3***
Bonvin	—	—	**	**	0	***	***	0	0	5/3**/2***
ClusPro	**	0	0	0	***	*	0	0	*	5/2**/1***
Sternberg	**	0	0	*	*	0	**	0	*	5/2**
Eisenstein	***	0	0	*	***	0	**	0	0	4/1**/2***
Ritchie	0	0	0	**	***	*	*	0	0	4/1**/1***
Zhou	—	—	0	—	***	**	*	*	0	4/1**/1***
Ten Eyck	0	0	0	0	***	***	**	0	0	3/1**/2***
Zacharias	**	0	—	—	—	—	***	0	**	3/2**/1***
Valencia	*	0	0	*	*	—	0	0	—	3
Vakser	—	—	0	—	—	—	**	**	0	2/2**
Umeyama	0	0	0	**	*	0	0	0	0	2/1**
Kaznessis	—	—	0	0	***	0	0	0	0	1/1***
Fano	—	—	0	*	0	0	0	0	0	1
Gottschalk	—	—	—	*	—	—	—	—	—	1
Palma	0	0	0	—	0	0	0	0	0	1
Poupon	—	—	—	—	0	*	0	0	0	1
Wang	0	0	0	*	0	0	0	0	0	1
Target summary	11/7**/2***	1	4/1**	15/7**	16/11***	10/2**/4***	14/7**/5***	7/6**	10/4**/1***	

This table summarizes the results obtained by all the groups that submitted one or more predictions of acceptable quality or better for at least one target.

Column 1 lists the name of the principal investigator. The next 9 columns list the results obtained for each of the 9 targets. The right-most column summarizes the results per predictor group, and the bottom row summarizes the results per target.

'0' indicates that none of the submitted predictions was of acceptable quality. '—' indicates that no predictions were submitted. '*' indicates that at least one of the submitted predictions was in the acceptable range, '**' indicates that at least one of the submitted predictions was of medium accuracy, and '***' indicates that at least one prediction was of high accuracy. See the text as well as Ref. 11 for the definition of the parameters range used to rank the predictions.

The summary entries list the total number of acceptable predictions, followed by the number of predictions of medium and high accuracy denoted by a '**' and '***', respectivley.

This notwithstanding, we see that 2 groups (Abagyan and Wolfson) managed to submit correct predictions of 8 out of the 9 evaluated targets, an altogether impressive performance. The Abagyan group produced overall better quality predictions, with high-accuracy models for 2 targets and medium-accuracy ones for 4 targets. The Wolfson group's results included medium-accuracy models for 3 targets, and acceptable models for the remaining 5 targets.

The next-best ranking predictor groups with an excellent success score are those of Weng and Bates. Both produced correct predictions for 7 targets. Those of Weng and colleagues were of higher accuracy, including 3 targets with high-accuracy and 3 with medium-accuracy models. Of the models produced by the Bates group, only 3 were of medium accuracy. A very good performance is displayed by the groups of Baker and Camacho, with each submitting correct predictions for 6 targets. Of those, 4 targets were predicted with high accuracy by the Baker group, and 2 were predicted at high accuracy by the Camacho group. The Gray, Bonvin, and Sternberg groups together with the server ClusPro come next, with correct predictions for 5 targets. It is noteworthy

that ClusPro is a fully automatic Web server producing predictions without human intervention.

A further 3 groups submitted correct predictions for 4 targets, including at most 2 high-accuracy predictions. The remaining groups had 3 or less targets correctly predicted.

Together these results indicate that groups such as Abagyan, Wolfson, Weng, and Bates are among the top performers. All 4 groups have appreciable experience in the development of protein–protein docking methods and continue to improve them. It is on the other hand very encouraging to see that other groups, such as those of Baker and Gray, who joined the field more recently, contributing new sampling and/or scoring methods, but did participate in previous rounds of CAPRI, are catching up fast. Results obtained by groups such as that of Bonvin, which are relative newcomers the field, and by the server ClusPro, can also be considered as very promising.

Last, it should be emphasized that the lower performance scores of some of the groups may not necessarily reflect the quality of their approach, because, as inspection of Table II clearly indicates, a good number of these groups did not submit predictions for every target.

THE DOCKING PROCEDURES: WHAT IS NEW?

The notable improvements in the prediction performance for Rounds 3–5 of CAPRI despite the significant difficulty presented by some of the targets, seem to indicate that progress is being made in docking methods, with CAPRI acting as a catalyst.

To which of the methods, or methodological aspects, can this progress be attributed?

In the present section we try to answer this question by briefly reviewing the most salient new developments in docking procedures used by the groups whose predictions we evaluated. These include new approaches introduced by several groups that recently joined the CAPRI experiments, as well as improvements made to existing methods by more veteran groups.

Table III provides an overview of these new developments. Table III(A) summarizes some of the more successful new and improved methods, as judged by their performance in CAPRI Rounds 3–5. Table III(B) lists other novel methods, most in their very early stages of development, which performed less well. Given the obvious difficulty in providing an accurate review in such a limited space, readers are referred to the original articles for details.

Inspection of Table III(A), and comparison with the Methods Table of the first CAPRI evaluation report,[11] reveals that the major novel aspects deal with the treatment of side-chain and backbone conformational flexibility.

Side-Chain Flexibility

Quite some progress has been achieved in recent years in the ability of protein structure prediction methods, both of the ab initio and homology modeling category, to model side-chain conformations. When the backbone conformation is that of the native protein or is close to it (≤ 1 Å RMSD), side-chain conformations of buried residues can be predicted quite accurately: to ~ 1 Å RMSD of those in the crystal structure.[40] There is therefore no reason why similar accuracy should not be achieved for side-chains in interfaces of correctly docked complexes, provided the backbone conformations of the components have either changed little or have been correctly modeled.

It is therefore quite satisfying to see that an increasing number of groups are now successfully carrying out the task of side-chain modeling. The majority of the methods in Table III(A) include a step for optimizing side-chain conformations, but the individual optimization procedures vary substantially. Groups like those of Baker and Gray (who use different versions of the same docking software), as well as the Bates and Abagyan groups, sampled a wide range of side-chain conformations by different strategies. Baker and Gray performed sampling of side-chain rotamers,[28] followed by energy minimization, an approach shown to work well in protein structure predictions[41,42] and in protein design calculations.[43,44] Sternberg and colleagues used a multiple copy refinement technique,[45] which also samples multiple conformations of side-chains but by a modified mean-field approach. Abagyan combines pseudo-Brownian Monte Carlo minimization with a biased probability global side-chain placement on a grid poten-

tial.[21,46,47] Bonvin and colleagues performed simulated annealing starting from several side-chain conformations for each residue,[24] whereas the remaining groups in Table III(A), who treat side-chain flexibility, performed a short step of molecular dynamics (MD) simulation (Camacho and Gatchell[25]) or energy minimization (Ritchie,[29] Weng and colleagues[31]), both of which involve only a limited explorations of conformational space. The method by Zacharias is the only one to incorporate side-chain flexibility at the docking step, with promising results.[34]

An indication on how well the different procedures model side-chain conformations in the predicted complexes can be obtained from the inspection of Figure 3, which plots for each target the RMSDs of side-chain atoms (Cβ and beyond) and backbone atoms, respectively, computed for models of acceptable quality or better, submitted by the different groups. The side-chain RMSDs were computed following the optimal superposition of the side-chain atoms belonging to interface residues, with the latter as defined above in the assessment protocol. As expected, the side-chain RMSD values are strongly linearly correlated with those of the backbone atoms, with a slope close to 1, but a variable intercept ranging from 0.3 to 1.5, which indicates that that the side-chain RMSD values are always higher than those of the backbone, but to a varying degree that depends on the target. We see that side-chain conformations are in general modeled to within about 1–1.5 Å RMSD in all high accuracy solutions—those with I-rms (backbone RMSD) of 0.5 Å or less. Interestingly, excellent side-chain models are provided by the server ClusPro and the Eisenstein and Weng groups for T08. Bonvin, Baker, Camacho, and Ten Eyck also produced accurate side-chain conformations for T13, and Abagyan, Baker and Zacharias produced high-quality side-chain models for T14. Given the clear progress made in side-chain modeling, a more detailed assessment based on the actual values of the side-chain dihedral angles will in the future be performed as part of the CAPRI evaluation protocol.

Backbone Flexibility

Adequate treatment of backbone flexibility remains a major challenge for all protein modeling tasks, even when those do not require complete rebuilding of the polypeptide chain. This is the case for homology modeling,[48] sequence design,[43] and hence also for docking. In comparison with the situation in CAPRI 2 years ago, many more groups are attempting to meet this challenge. The Gray group introduces a global refinement step as part of the procedure of side-chain rotamer sampling, which produces incremental small backbone adjustments every time a set of new rotamer conformations is introduced. The Abagyan and Weng groups use global refinement as a final step before ranking the docking solutions, enabling only small backbone adjustments. The Bates and Bonvin groups perform docking on multiple conformations of the components, which are derived from a principal component analysis coupled to MD simulations (the Bates group, for some targets), from snapshots of MD simulations or from NMR

TABLE III. Novel and Improved Protein–Protein Docking Methods

A. Successful novel methods and recent improvements on existing methods

Participants	Sampling[a]	Scoring function[b]	Backbone flexibility[c]	Side-chain flexibility[c]	Availability	Oligomerization symmetry	Reference
Abagyan	PSB-MC	^{d}(K) ^{r}(Θ) ^{dr}(W C H Φ G)	No	On a grid potential (^{r})	**ICM-DISCO** (cl) http://www.molsoft.com	Variable linkage of equivalent monomer	Fernandez-Recio et al.[21]
Baker	MC	^{d}(R) ^{r}(W G HΘ C K) ^{dr}(P)	No	Rotamer lib & off-rotamer sampling (^{dr})	**Modified** RosettaDock (fal) http://graylab.jhu.edu/docking/rosetta/	Homo-N-mer generation by symmetry Orientation filter	Wang et al.[22]
Bates	MV, FFT, Euler	^{d}(Z) ^{dr}(W P R K) ^{dr}(C)	MD, MD + PCA	Side-chain multicopy flexible refinement force field (^{r})	**Modified** FT_DOCK	Orientation filter	Smith et al.[23]
Bonvin	EM + MV + MS	^{r}(K) ^{dr}(R W C)	^{pd}(NMR, MD) ^{r}(SA-MV + MS)	^{pd}(NMR, MD) ^{r}(SA-MV + MS)	**HADDOCK** (fal) http://www.nmr.chem.uu.nl/haddock	Explicit symmetry restraints with N-body docking	Dominguez et al.[24]
Camacho	FFT	^{r}(W K) ^{dr}[Z G C (P)]	No	^{pd}(short MD)	**SmoothDock**	Homo-N-mer generation by symmetry	Camacho et al.[25]
ClusPro	FFT	^{r}(K) ^{dr}[Z G C (P)]	No	No	**ClusPro** (www) http://nrc.bu.edu/cluster/	Homo-N-mer generation by symmetry	Comeau et al.[26]
Eisenstein	FFT	^{d}[Z R (C) Φ K]	No	No	**MolFit** http://www.weizmann.ac.il/Chemical_Research_Support//molfit/	Orientation filter and monomer assembly by symmetry; intradomain assembly	Berchanski et al.[27]

TABLE III. (Continued)

A. Successful novel methods and recent improvements on existing methods

Participants	Sampling[a]	Scoring function[b]	Backbone flexibility[c]	Side-chain flexibility[c]	Oligomerization symmetry	Availability	Reference
Gray	MCM	^{d}(R P) ^{r}(W G H Θ C K)	No	Rotamer library(^{r})	No	**RosettaDock** (fal) http://graylab.jhu.edu/docking/rosetta/	Gray et al.[28]
Ritchie	PF	^{d}(R) ^{r}(W H K) ^{dr}(Z C)	No	No	Homo-N-mer generation by symmetry	**Hex** (b,fal) http://www.csd.abdn.ac.uk/hex/	Ritchie et al.[29]
Sternberg	FFT	^{d}(Z) ^{r}(P R K W) ^{dr}(C)	No	Optimizing full atoms vdw and electrostactics energy (^{r})	No	**3D_DOCK** http://www.sbg.bio.ic.ac.uk/docking/	Aloy et al.[30]
Weng	FFT	^{d}(Z) ^{r}(W T C G)	Optimizing full atoms internal energy and vdw (^{r})	Optimizing full atoms internal energy and vdw (^{r})	Home-N-mer generation by symmetry	**ZDOCK + RDOCK** (fal) http://zdock.bu.edu/software.php	Li et al.[31]
Wolfson	Geometric docking	^{d}[Z K (R)] ^{r}[(PH)]	Hinges	No, a bit of clashing (^{d})	Homo-N-mer generation by symmetry	**PatchDock** (www) http://bioinfo3d.cs.tau.ac.il/PatchDock/ **FlexDock** **SymmDock** (www) http://bioinfo3d.cs.tau.ac.il/SymmDock/	Schneidman et al.[32,33]
Zacharias	Euler	^{d}(W Φ R) ^{r}(C W)	No	2 pseudo-atoms–side-chain multicopy (^{d})	No	**ATTRACT**	Zacharias et al.[34]

TABLE III. (Continued)

B. Novel methods still under development

Participants	Sampling[a]	Scoring function[b]	Backbone flexibility[c]	Side-chain flexibility[c]	Oligomerization symmetry	Availability	Reference
Fano	PF + PCA MIF	[d](Φ) [r](H W) [dr](Z C)	No	No	No	**GridHex**	Fano et al.[35]
Kaznessis	FFT	[r](W C G) [dr](Z P R)	No	[r](EM)	No		Duan et al.[36]
Lee	CSA	[r](K R) [dr](W C Θ)	No	No	No	Tinker (fl)	Lee et al.[37]
Mustard	Polar Fourier	[r](R H K) [dr](Z C W)	ED + PCA ([r])	ED + PCA ([r])	No	http://dasher.wustl.edu/tinker/ **ED-Hex**	Mustard & Ritchie[38]
Poupon	Euler + Voronoi	[r](IA VV VD)	No	No	No		Bernauer et al.[39]

[a]PSB, Pseudo–Brownian dynamics; EM, energy minimization; MC, Monte Carlo sampling; MCM, Monte Carlo minimization; MV, Molecular dynamics in vacuum; MS, Molecular dynamics in explicit solvent; FFT, Fast Fourier Transform; PF, Polar Fourier Transform; Euler, optimization of the Euler angles; PCA, principal component analysis; MIF, for molecular interactions fields; CSA, conformation space annealing; Voronoï, Voronoï tessellations.

[b]C, general electrostatics; Φ, hydrophobic potential; G, desolvation energy; H, hydrogen bond potential; K, clustering; P, contact pair potential; PH, graph theory; R, experimental restraints or residue conservation; Θ, rotamer probability; W, van der Waals potential; VV, Voronoï volumes; VD, Voronoï distance; Z, shape complementarity.

[c]SA, simulated annealing; EM, energy minimization; NMR, nucleic magnetic resonance ensembles; ED, essential dynamics.

This table summarizes the recent new developments in docking procedures used by CAPRI participants: (a) successful novel methods and improved versions of existing methods and (b) novel methods still in development.

Column 1 lists the first name of the principal investigator as for Tables I and II. Column 2 lists the sampling method used in the docking process for each of them. For the acronyms see the footnote. Any of these terms for the scoring functions appearing between brackets means that it is not always used, i.e., depending on the rigid-body sampling algorithm. Since the different scoring terms might be applied at different docking stages, we group them using the following tags: '[d]( )', when the scoring terms are used at the sampling stage; '[r]( )', when the scoring terms are used at the refinement stage and '[dr]( )' when they are used at both stages. Columns 4, 5, and 6 list the special treatment for protein backbone flexibility, side-chain flexibility, and oligomer symmetry, respectively. When two techniques appear between '–' means that they are applied sequentially. '[pd]', means that flexibility is considered prior to docking; '[d]', flexibility is considered at the sampling step; '[r]', means that flexibility is considered at the refinement step, and '[dr]', means that it is considered at the sampling and the refinement steps. Column 7 lists the name of the algorithm, usually the name of the program that implements it. In Courier normal, when the docking algorithm is implemented in a program that is not developed by the participant; in Times bold, otherwise. Between brackets the program is available under a free academic license (usually the source code), 'fl' means that the program is a free license, for all user commercial an academic under certain conditions from the developers, 'www' means that the program is implemented in a web server and 'b' means that only binary executables of the program are provided. In any of those cases, a web link, when available, is provided for downloading, web utilization or just information browsing of the program. The last column, 8, lists the most recent bibliographic reference of each method.
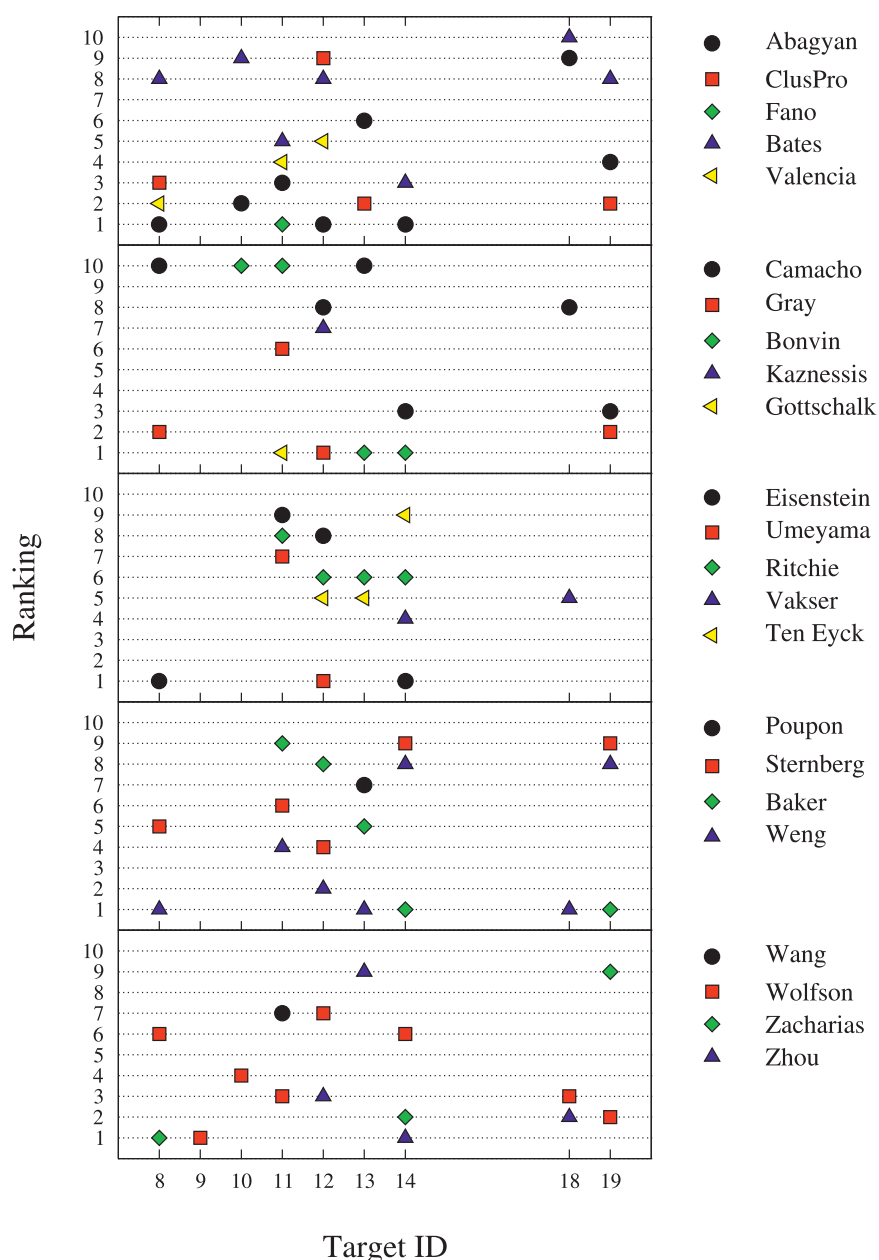
Participant's Ranking of Best Predictions

Fig. 4. Participant ranking of best predictions. The rank given by each participant to the best scoring model is plotted against the target identifier. Only models acceptable or better are considered. Among the models of the same quality, whether "high" or "medium" or "acceptable," the best scoring model is taken as the one with the highest f_{nat}. The ranking of participants were grouped so as to minimize overlaps of points on the graphs.

conformations, followed by simulated annealing including side-chain atoms in a first step, and both side-chain and backbone atoms in a second step (Bonvin). These latter methods can produce somewhat larger structural deformations than the energy minimization methods, but those deformations are generally limited to those with low-energy barriers that are accessible during very short timescales to individual components of the complex.

The approaches of the Eisenstein and Wolfson groups are on the other hand designed to handle conformational changes of any size, but preferably those involving relative movements of whole domains. When a subunit is known or suspected to undergo conformational change, it is subdivided into domains or fragments, the fragments are docked independently and the docked fragments are assembled, in a similar fashion to some of the in silico small-molecule

docking algorithms.[32,49] The problem with this approach is that choices need to be made on how to best subdivide the protein structure, usually in absence of any evidence.

Lastly, we see that none of the methods in Table III(B) denoted as "under development" of groups that participated in the last 3 rounds of CAPRI seem as to tackle backbone flexibility. An exception is a new method by Mustard and Ritchie,[38] which uses an "essential dynamics" approach and polar Fourier Transform to dock multiple protein conformations.

Sampling Procedures and Treatment of Symmetry

Sampling the relative orientations of the ligand and receptor molecules is a key step of any docking procedure. It is usually the first step in which a very large number of possible solutions must be efficiently and reliably evaluated, so that very unlikely solutions can be eliminated, leaving a tractable number of candidates for subsequent analysis. Hence, for computational efficiency, the sampling step is usually performed using a very simplified model of the protein structures and a correspondingly simple scoring function.

A good fraction of the methods listed in Table III [6 out of 13 in Table III(A), and 1 out of 5 in Table III(B)], use FFT-based algorithms, which together with the geometric hashing and the polar Fourier Transform techniques, remain the fastest and therefore the most efficient procedures for sampling relative receptor–ligand orientations. Several of the alternative procedures, such as Monte Carlo sampling (MC) (Bonvin, and Gray and Baker groups) or systematic searches using polar coordinates ("Euler" in Table III), seem to be less efficient. A few completely novel methods such as conformational space annealing (CSA) by Lee et al.[37] and the molecular interaction field (MIF) by Fano and colleagues[35] were also introduced [Table III(B)].

In order to choose the subset of solutions that will undergo subsequent analysis, a majority of the groups cluster the solutions into families of similar structures and select representatives from the most populated clusters for further analysis. The Baker and Gray groups also analyze the energy (score) spectrum of the solutions obtained in the first coarse sampling step, and look for one or a few solutions having significantly lower energy than the bulk of the remaining ones. Subsequent side-chain building and global refinement steps concentrate on these solutions. When no such solutions are found, the coarse search step is repeated from different starting positions.

Last, a fair number of groups [all except Gray, Sternberg, and Zacharias in Table III(A)] have introduced procedures for docking identical subunits into symmetrical assemblies. Such procedures introduce specific dependencies between the rigid-body degree of freedom, whose effect is to reduce the number of independent parameters from 6 to 4.[50]

Scoring Functions

As in previous rounds of CAPRI, a wide range of scoring functions is used by predictors (see Table III). A good number of methods still rely on shape complementarity measures, but those are in general supplemented with other terms (e.g.,van der Waals, Coulomb, desolvation). The use of scoring functions that combine various terms is the rule. These can include rotamer probabilities, contact pair potentials, as well as experimental restraints (see below). Several novel scoring functions, with parameters computed from or fitted to known complexes, were also tested, including one knowledge-based statistical potential[51] and one based on Voronoï tessellation (Bernauer et al.[39]). The latter affords a measure of the packing of interface atoms, a quantity that has hitherto not been exploited in docking.

Use of Prior Knowledge

An important ingredient for achieving successful docking remains the use of prior knowledge of the protein regions that are likely to interact. Such knowledge includes indications on interacting residues from published biochemical or mutagenesis studies. With the increasing availability of information on protein sequences and 3D structures, however, predictors can themselves derive information on protein regions likely to interact by mapping patterns of sequence conservation across related proteins onto the 3D structure of the individual protein components. This information has been used with a remarkable success rate, either as "experimental restraints" to guide the search or in order to filter out solutions, and has become an integral component of docking procedures.

Ranking the Solutions by the Predictors: How Effective Is It?

The model number listed in the leftmost column of Table I represents the position of the model in the ranked list of 10 predictions submitted by the predictors for each target. Many predictors produce this rank purely on the basis of the particular scoring scheme that they use. Some however, trust less their scoring function and use ad hoc criteria. In either case, the rank of the prediction generally reflects the degree of confidence that predictors have in the submitted model, with high-confidence models appearing at top of the list.

Figure 4, which surveys the rank of the best prediction provided by each group for each of the 9 targets evaluated here, shows that only 1 group (Abagyan) provided a prediction with rank 5 or less for 6 out of the 9 targets. Two groups (Weng and Wolfson) provided a prediction with rank 5 or less for 5 out of the 9 targets. Three groups (Baker, Gray and Zhou) and the ClusPro server provided a prediction with rank 5 or less for 3 out of 9 targets. The ranking provided by the remaining participants seem to be significantly less reliable.

One should recall, however, that the 10 submitted predictions already represent the choice of a very small number of solutions that were selected from an extremely large number of tested possibilities. Depending on how the selection is performed and how fine-grained the clustering of similar solutions is, meaningful ranking of the 10 submitted models may or may not be feasible. This is an

issue that predictors will have to investigate in future CAPRI rounds.

WHERE DO WE GO FROM HERE?

This second evaluation report of the CAPRI predictions, demonstrates clearly that progress is being achieved in protein–protein docking procedures. Despite the different challenges that each of the targets evaluated here posed to prediction methods, all were predicted by at least 1 group, and often by many. Furthermore, for a good number of targets, high-accuracy models could be produced.

This very encouraging result can be attributed in part not only to the participation of new groups, contributing completely new procedures, but also to incremental improvements of scoring functions and to the manner in which additional information (biochemical or sequence conservation) is exploited in order to filter out the many false-positive solutions invariably generated by all docking procedures.

It is particularly encouraging to see that many predictors do not shy away from trying out new, inventive approaches for tackling backbone and side-chain flexibility, including the mixing and matching of different scoring functions and sampling procedures. Another promising development is the successful use of homology-built models in docking. All 3 targets in which 1 component was built from the structure of a related protein were rather well predicted. Groups familiar with homology modeling methods had a clear advantage over classical dockers, but this advantage will fade away as powerful Web services for homology modeling become available.

CAPRI is clearly playing an important role in fostering these developments, and the improvements in the performance of docking procedures that they seem to bring are a strong incentive to continue with the CAPRI experiment. To maintain the momentum created by CAPRI, we need a steady supply of new targets, and we therefore call upon X-ray crystallographers and NMR experts to trust us with their structures. The submission of a target to CAPRI does not jeopardize the confidentiality of the work, since submitted atomic coordinates remain confidential until released by the author or by the PDB. On the other hand, it contributes to progress in docking procedures and enhances visibility of the work done by the structural biologists.

REFERENCES

1. Ho Y, Gruhler A, Heilbut A, Bader GD, Moore L, Adams SL, Millar A, Taylor P, Bennett K, Boutilier K, Yang L, Wolting C, Donaldson I, Schandorff S, Shewnarane J, Vo M, Taggart J, Goudreault M, Muskat B, Alfarano C, Dewar D, Lin Z, Michalickova K, Willems AR, Sassi H, Nielsen PA, Rasmussen KJ, Andersen JR, Johansen LE, Hansen LH, Jespersen H, Podtelejnikov A, Nielsen E, Crawford J, Poulsen V, Sorensen BD, Matthiesen J, Hendrickson RC, Gleeson F, Pawson T, Moran MF, Durocher D, Mann M, Hogue CW, Figeys D, Tyers M. Systematic identification of protein complexes in *Saccharomyces cerevisiae* by mass spectrometry. Nature 2002;415:180–183.
2. Gavin AC, Bosche M, Krause R, Grandi P, Marzioch M, Bauer A, Schultz J, Rick JM, Michon AM, Cruciat CM, Remor M, Hofert C, Schelder M, Brajenovic M, Ruffner H, Merino A, Klein K, Hudak M, Dickson D, Rudi T, Gnau V, Bauch A, Bastuck S, Huhse B, Leutwein C, Heurtier MA, Copley RR, Edelmann A, Querfurth E, Rybin V, Drewes G, Raida M, Bouwmeester T, Bork P, Seraphin B, Kuster B, Neubauer G, Superti-Furga G. Functional organization of the yeast proteome by systematic analysis of protein complexes. Nature 2002;415:141–147.
3. Claverie JM. Gene number: what if there are only 30,000 human genes? Science 2001;291:1255–1257.
4. Uetz P, Giot L, Cagney G, Mansfield TA, Judson RS, Knight JR, Lockshon D, Narayan V, Srinivasan M, Pochart P, Qureshi-Emili A, Li Y, Godwin B, Conover D, Kalbfleisch T, Vijayadamodar G, Yang M, Johnston M, Fields S, Rothberg JM. A comprehensive analysis of protein–protein interactions in *Saccharomyces cerevisiae*. Nature 2000;403:623–627.
5. Edwards AM, Kus B, Jansen R, Greenbaum D, Greenblatt J, Gerstein M. Bridging structural biology and genomics: assessing protein interaction data with known complexes. Trends Genet 2002;18:529–536.
6. Sali A, Glaeser R, Earnest T, Baumeister W. From words to literature in structural proteomics. Nature 2003;422:216–225.
7. Chance MR, Fiser A, Sali A, Pieper U, Eswar N, Xu G, Fajardo JE, Radhakannan T, Marinkovic N. High-throughput computational and experimental techniques in structural genomics. Genome Res 2004;14:2145–2154.
8. Venclovas C, Zemla A, Fidelis K, Moult J. Assessment of progress over the CASP experiments. Proteins 2003;53(Suppl 6):585–595.
9. Janin J, Henrick K, Moult J, Eyck LT, Sternberg MJE, Vajda S, Vakser I, Wodak SJ. CAPRI: a Critical Assessment of PRedicted Interactions. Proteins 2003;52:2–9.
10. Wodak SJ, Méndez R. Prediction of protein–protein interactions: the CAPRI experiment, its evaluation and implications. Curr Opin Struct Biol 2004;14:242–249.
11. Méndez R, Leplae R, De Maria L, Wodak SJ. Assessment of blind predictions of protein–protein interactions: current status of docking methods. Proteins 2003;52:51–67.
12. Janin J. The targets of CAPRI Rounds 3–5. Proteins 2005;60:170–175.
13. Takagi J, Yang Y, Liu JH, Wang JH, Springer TA. Complex between nidogen and laminin fragments reveals a paradigmatic beta-propeller interface. Nature 2003;424:969–974.
14. Terrak M, Kerff F, Langsetmo K, Tao T, Dominguez R. Structural basis of protein phosphatase 1 regulation. Nature 2004;429:780–784.
15. Lo Conte L, Chothia C, Janin J. The atomic structure of protein–protein recognition sites. J Mol Biol 1999;285:2177–2198.
16. Vajda S. Classification of protein complexes based on docking difficulty. Proteins 2005;60:176–180.
17. Kraulis P. MOLSCRIPT: a program to produce both detailed and schematic plots of protein structures. J Appl Crystallogr 1991;24:946–950.
18. Sanner MF, Olson AJ, Spehner JC. Reduced surface: an efficient way to compute molecular surfaces. Biopolymers 1996;38:305–320.
19. Merritt E, Bacon, DJ. Raster3D: photorealistic molecular graphics. Methods Enzymol 1997;277:505–524.
20. McLachlan A. rapid comparison of protein structures. Acta Crystallogr 1982;A38:871–873.
21. Fernandez-Recio J, Totrov M, Abagyan R. Identification of protein–protein interaction sites from docking energy landscapes. J Mol Biol 2004;335:843–865.
22. Wang C, Schueler-Furman O, Baker D. Improved side-chain modeling for protein–protein docking. Protein Sci 2005; 14:1328–1339.
23. Smith GR, Sternberg MJE, Bates PA. The relationship between the flexibility of proteins and their conformational states on forming protein–protein complexes with application to protein–protein docking. J Mol Biol 2005;347:1077–1101.
24. Dominguez C, Boelens R, Bonvin AM. HADDOCK: a protein–

protein docking approach based on biochemical or biophysical information. J Am Chem Soc 2003;125:1731–1737.

25. Camacho CJ, Gatchell DW. Successful discrimination of protein interactions. Proteins 2003;52:92–97.

26. Comeau SR, Gatchell DW, Vajda S, Camacho CJ. ClusPro: an automated docking and discrimination method for the prediction of protein complexes. Bioinformatics 2004;20:45–50.

27. Berchanski A, Shapira B, Eisenstein M. Hydrophobic complementarity in protein–protein docking. Proteins 2004;56:130–142.

28. Gray JJ, Moughon S, Wang C, Schueler-Furman O, Kuhlman B, Rohl CA, Baker D. Protein–protein docking with simultaneous optimization of rigid-body displacement and side-chain conformations. J Mol Biol 2003;331:281–299.

29. Ritchie DW. Evaluation of protein docking predictions using Hex 3.1 in CAPRI rounds 1 and 2. Proteins 2003;52:98–106.

30. Aloy P, Querol E, Aviles FX, Sternberg MJE. Automated structure-based prediction of functional sites in proteins: applications to assessing the validity of inheriting protein function from homology in genome annotation and to protein docking. J Mol Biol 2001;311:395–408.

31. Li L, Chen R, Weng Z. RDOCK: refinement of rigid-body protein docking predictions. Proteins 2003;53:693–707.

32. Schneidman-Duhovny D, Inbar Y, Nussinov R, Wolfson HJ. Geometry-based flexible and symmetric protein docking. Proteins 2005;60:224–231.

33. Schneidman-Duhovny D, Inbar Y, Nussinov R, Wolfson HJ. PatchDock and SymmDock: servers for rigid and symmetric docking. Nucleic Acids Res 2005. Forthcoming.

34. Zacharias M. Protein–protein docking with a reduced protein model accounting for side-chain flexibility. Protein Sci 2003;12:1271–1282.

35. Fano A, Carrieri A, Ritchie D. Improving the scoring of protein–protein interactions by means of surface complementarity and molecular interaction fields: the GridHex approach. Manuscript in preparation.

36. Duan Y, Reddy BV, Kaznessis YN. Physicochemical and residue conservation calculations to improve the ranking of protein–protein docking solutions. Protein Sci 2005;14:316–328.

37. Lee K, Czaplewski C, Kim SY, Lee J. An efficient molecular docking using conformational space annealing. J Comput Chem 2005;26:78–87.

38. Mustard D, Ritchie DW. Docking essential dynamics eigenstructures. Proteins 2005;60:269–274.

39. Bernauer J, Poupon A, Azé J, Janin J. A docking analysis of the statistical physics of protein–protein recognition. Phys Biol 2005;2:S17–S23.

40. Canutescu AA, Shelenkov AA, Dunbrack RL Jr. A graph-theory algorithm for rapid protein side-chain prediction. Protein Sci 2003;12:2001–2014.

41. Rohl CA, Strauss CE, Misura KM, Baker D. Protein structure prediction using Rosetta. Methods Enzymol 2004;383:66–93.

42. Rohl CA, Strauss CE, Chivian D, Baker D. Modeling structurally variable regions in homologous proteins with Rosetta. Proteins 2004;55:656–677.

43. Jaramillo A, Wodak SJ. Computational protein design is a challenge for implicit solvation models. Biophys J 2005;88:156–171.

44. Ogata K, Jaramillo A, Cohen W, Briand JP, Connan F, Choppin J, Muller S, Wodak SJ. Automatic sequence design of major histocompatibility complex class I binding peptides impairing CD8+ T cell recognition. J Biol Chem 2003;278:1281–1290.

45. Jackson RM, Gabb HA, Sternberg MJE. Rapid refinement of protein interfaces incorporating solvation: application to the docking problem. J Mol Biol 1998;276:265–285.

46. Fernandez-Recio J, Totrov M, Abagyan R. ICM-DISCO docking by global energy optimization with fully flexible side-chains. Proteins 2003;52:113–117.

47. Totrov M, Abagyan R. Detailed ab initio prediction of lysozyme–antibody complex with 1.6 Å accuracy. Nat Struct Biol 1994;1:259–263.

48. Kopp J, Schwede T. Automated protein structure homology modeling: a progress report. Pharmacogenomics 2004;5:405–416.

49. Berchanski A, Eisenstein M. Construction of molecular assemblies via docking: modeling of tetramers with D2 symmetry. Proteins 2003;53:817–829.

50. Pierce B, Tong W, Weng Z. M-ZDOCK: a grid-based approach for Cn symmetric multimer docking. Bioinformatics 2005;21:1472–1478.

51. Zhang C, Liu S, Zhou Y. Accurate and efficient loop selections by the DFIRE-based all-atom statistical potential. Protein Sci 2004;13:391–399.